Models for correlated multifractal hypersurfaces

D. M. Tavares and L. S. Lucena
International Center for Complex Systems and Departamento de Física Teórica e Experimental—UFRN, Natal-RN 59078-970, Brazil
(Received 12 August 2002; published 24 March 2003)

We discuss and implement computer approximations of fractal and multifractal hypersurfaces. These hypersurfaces consist of reconstructions of a stochastic process in the real space from randomly distributed variables in the discrete wavelet domain. The synthetic surfaces have the usual fractional Brownian motion as a particular case, and inherit the correlation structure of these fractals. We first introduce the one-dimensional version of these surfaces that obey a weak self-affine symmetry. This symmetry appears in the wavelet domain as a condition on the second moments of the probability distributions of the wavelet coefficients. Then we use these relations to define the fractals and multifractals in d dimensions. Finally, we concentrate on the generation of samples of these hypersurfaces.

DOI: 10.1103/PhysRevE.67.036702 PACS number(s): 95.75.Pq, 05.40.−a, 02.50.−r, 81.05.Rm

I. INTRODUCTION

In recent years, a widespread interest on fractal concepts and in their use to investigate irregular data from experiments and simulations on various complex systems has been noticed [1–4]. This interest is due to the recognition that the models based on differentiable manifolds are not well suited for the depiction of these harsh geometries. The fact is that the measured properties are extremely heterogeneous, and for this reason, any differentiable approximation has necessarily a large amount of parameters. This precludes their use for expressing the regularities through simple relations, or even for indicating the existence of regularities. Fractal concepts just apply more directly to the important aspects of these seemingly intractable geometries. These aspects are mainly connected with two themes: scaling and correlations. Due to chaos and roughness (nondifferentiability), probabilistic characterization is intrinsic to the methodology for studying such geometries, even when there are reasons to believe that the underlying mechanisms are deterministic. This is remarkably so in the investigation of fully developed turbulence, or more generally in dealing with strange attractors [5–9].

The existence of many cases in nature, where scale symmetries are present is a welcome fact. These cases had the foremost attention and were the most investigated because they are examples of the importance of the scale symmetries, and also because they are the simplest situations in which nondifferentiable models are the most suited. Nature give us some entry points to this difficult region when yielding to simple models such as the diffusion limited aggregation [10], percolation [11,12], or fractional Brownian motion (fBm) [13]. The applicability of these models to a variety of measured physical quantities indicates that the assumed simple scaling is in good agreement with the actual scaling in all these cases [1–4], i.e, it establishes that a fractal dimension d_f is a very common characteristic of complex patterns.

Following this evidence that nondifferentiability often appears in conjunction with scale invariance, the first kind of configurations to be considered were the fractal sets. Fractal models presenting deterministic or random self-similarity are nowadays a standard in situations where the system presents no characteristic scale. However, in important situations, the scaling properties of the system vary with position, and in these cases, it is necessary to use more complicated objects than a fractal [14–26]. In such systems, the scaling symmetry of fractals is broken by processes that involve interaction between scales giving rise to fluctuating cascades. The suitable nondifferentiable objects with inhomogeneous scaling for modeling these latter cases are the multifractals [27].

Multifractals are usually assimilated in the following construction [28–30]. Consider a set S (that can be a fractal), and balls $B_l(\mathbf{x})$ belonging to a covering of S having norm l. A multifractal measure scales as $\mu(B_l(\mathbf{x})) \sim l^{\alpha(\mathbf{x})}$, with a point dependent exponent giving the singularity strength. This justifies the introduction of a partition of the support composed of the sets $S_\alpha = \{\mathbf{x} \in S : \alpha(\mathbf{x}) = \alpha\}$. The sets S_α are fractals indicating the configuration of the singularities with strength α. Each set S_α has its own scaling properties, in part quantified by an exponent $f(\alpha)$ which was called the singularity spectrum. More precisely: let N_l be the number of balls in the covering of the support. Let $N_l(\alpha)$ be the number of balls that scales as l^α. This number scales as $N_l(\alpha) \sim N_l^{f(\alpha)} \sim l^{-f(\alpha)}$. *In summa*, the strength α gives the way μ scales at a point, and the spectrum $f(\alpha)$ gives the way the multiple fractal sets S_α scale. In a precise account, $f(\alpha)$ is the Hausdorff dimension of the set S_α [28]. A function $f: \mathbb{R}^d \to \mathbb{R}$ can also be treated in this way by associating to it a quantity defined in terms of a difference operator $\delta_{l,\mathbf{u}} f(\mathbf{x})$ or more generally in terms of wavelet transforms [31]. Here l is the norm of a covering with balls $B_l(\mathbf{x})$ as in the case of measures, and $\mathbf{u}$ is a fixed unit vector (we make a longer discussion on this directionality in Sec. III).

The multifractals are first examples of physically important stochastic fields, in which full scale symmetry is broken. A general and simple way to consider effects that break scale symmetries is through the study of probability distributions associated with the incremental process generating the considered stochastic fields. In particular, space-scale representations are immediate options to achieve such results, as we will argue, and we choose here the discrete wavelet transform, both for its simplicity and computational efficiency. However, the continuous wavelet transform (CWT) may be

employed as well [25,26,30,32]. Such an approach is needed because the usual search for spectra of scaling exponents, allowed by techniques as the multifractal formalism, lack the necessary generality, giving insufficient information to solve, for example, the inverse fractal problem [29]. The singularity spectrum is an important characteristic of the singular functions, in situations in which it can be determined. However, if we face the problem of characterizing the stochastic field, that is to say, of having a signature of it, the singularity spectrum is not enough. Moreover, it may not exist at all. There is, of course, strong motivation for the study of generalized scaling through exponents: the extension of the concept of universality to ample classes of physical systems without self-similarity; but one may expect in advance that this program has limitations. Then, it is clear that a way of characterizing the stochastic fields in general is necessary. It is important to be able to distinguish the fields, and have indication on their scaling, thus opening a main road to the topics of synthesis and simulation, as we will exemplify. The essential idea in our approach is that every stochastic field can be associated with definite probability distributions of wavelet coefficients, in the present case, discrete wavelet coefficients. To every scale indexed by j, we have a distribution P_j. If these distributions are known, one can generate approximations of samples of the stochastic field by inverse transformation of random variables in the wavelet domain.

Here, we use these notions as a background when introducing models for multifractal hypersurfaces. We assume that these hypersurfaces are similar enough to fBm to allow the measurement of Hurst exponents H. These models present the same nonlocal behavior of a fBm, i.e., the same two-point correlations, but do not fit in the same (non) differentiability class. In recent works, similar models were formulated in terms of cascade statistics that are applicable to turbulence and related phenomena [25,33]. Our models are instead parametrized by the Hurst exponents, and by conditions on the decay of the probability distribution functions (PDFs) of discrete wavelet coefficients. In the hypersurfaces considered in this paper, definite long range correlations or anticorrelations appear associated with multifractality. This also influences our method of analysis, which stresses a determination of the H exponent, to be followed by the detection of this multifractality. We point the connections of our procedures with the techniques based on the thermodynamical formalism, due to its role as a framework for important classes of multifractals.

The paper is organized as follows. Section II is devoted to the one-dimensional case and its properties. We present there various results that motivate our approach. In Sec. III, we discuss the generalization to d dimensions. We furnish there supplementary definitions and demonstrations, discuss the calculation of the singularity spectrum, and provide an algorithm for obtaining samples of the hypersurfaces. Section IV has some concluding remarks.

II. MODELS IN ONE DIMENSION

In the investigation of the so-called multifractal functions, a standard procedure is to determine their singularity spectrum $D(h)$, which is formally equivalent to the $f(\alpha)$ spectrum for singular measures. Here, $h=h(t)$ is a local regularity or Hurst exponent. Let $\Pi_H(t)$ represent the value of a random function Π_H at time t. This local exponent relates to the increments of the function through [30]

$$|\delta_l \Pi_H(t)| \sim l^{h(t)}, \tag{1}$$

where $\delta_l \Pi_H(t) \equiv \Pi_H(t+l) - \Pi_H(t)$. The singularity spectrum $D(h)$ is the Hausdorff dimension of the sets $S_h = \{t: h(t) = h\}$ [28]. This dimension defines how the joint probability density $p(h,l)$ of $|\delta_l \Pi_H(t)|$ scales with l [6],

$$p(h,l) \sim l^{1-D(h)}. \tag{2}$$

We assume that the symbol H represents the value of h, for which $D(h)$ is maximum. This means that H represents the more frequent singularity strength. Note that if the support of the function is $\mathbb{R}$, and if it is everywhere singular, then $D(H)=1$.

Since the importance of $D(h)$ was recognized in studies of turbulence, several methods have been developed for its measurement. The more elaborate ones consider the scaling exponents ζ_q of structure functions [27]

$$S_q(l) \equiv \int dt\, |\delta_l \Pi_H(t)|^q, \tag{3}$$

or, more recently, the scaling exponents τ_q of the partition function

$$Z_q(l) \equiv \sum \max |\langle \psi_{l,t} | \Pi_H \rangle|^q, \tag{4}$$

where $\langle \psi_{l,t} | \Pi_H \rangle$ is a CWT of Π_H [29,30]. The method based on the CWT singles out, at every scale l, the places where the modulus of the CWT reaches local maxima. Then a skeleton of lines of maxima is constructed from large to small scales. The sum in Eq. (4) is calculated on this skeleton only. The spectrum $D(h)$ is found from Legendre transforms of ζ_q, or τ_q. The technique is as follows. Due to the nonhomogeneous fractality, in the limit $l \to 0$, one can write $Z_q(l)$ in the asymptotic form

$$Z_q(l) \sim \int d\mu(h) l^{[hq - D(h)]}. \tag{5}$$

The term with the minimum exponent predominates, so we arrive at the Legendre transform

$$\tau_q = \min_h [hq - D(h)] \tag{6}$$

that can be inverted to give

$$D(h) = \min_q [hq - \tau_q]. \tag{7}$$

By this device, we have the spectrum in terms of the exponents τ_q. The same argument holds when using structure functions. The distinctive feature of a strictly multifractal motion is that the support of $D(h)$ has more than one element. In the thermodynamical formalism, this leads to non-

linear dependences of ζ_q or τ_q with q. General conditions and some criticism with respect to this technique can be found in Refs. [34,35]. The multifractal formalism for functions is built on such quantities as $|\delta_l f(t)|$ or $|\langle \psi_{l,t}|f\rangle|$, denoted as μ_f. Considering the multifractal as a stochastic process, μ_f is to be seen as a definition of its incremental process in the sense that

$$\mu_f \equiv \Pi_H * \Psi_{lt}, \tag{8}$$

where Ψ_{lt} is a filter that cuts off any divergence in the low frequency power spectrum of Π_H, l is an increment parameter (scale), t is a location parameter, and the star means convolution. In the case of fBm, wavelets and the increment operator are examples of such filters [36].

We wish to study a class of multifractal motions Π_H that possess a weakened form of self-affinity. The Π_H motions we are concerned here satisfy the following assumptions. First, they have the ensemble average

$$\overline{|\delta_l \Pi_H|^2} = \sigma_H^2 l^{2H}. \tag{9}$$

Second,

$$\Pi_H(0) = 0. \tag{10}$$

From these assumptions, it follows that the two-point correlation of the Π_H motion is

$$\overline{\Pi_H(t)\Pi_H(s)} = \frac{\sigma_H^2}{2}(|t|^{2H} + |s|^{2H} - |t-s|^{2H}). \tag{11}$$

This motion can be seen as a generalization of fBm that do not have zero mean, nor Gaussian statistics. The first consequence is that the motion is not statistically self-affine in general. Indeed, one easily proves from Eq. (11) that

$$\overline{\Pi_H(ct)\Pi_H(cs)} = \overline{c^H \Pi_H(t) c^H \Pi_H(s)}, \tag{12}$$

i.e., the motion $\Pi_H(ct)$ has the same two-point correlation as the motion $c^H \Pi_H(t)$. When the motion is self-affine, Eq. (12) holds necessarily, but the converse is not true. In fact, for the self-affine case, we have the stronger property

$$\Pi_H(ct) = c^H \Pi_H(t), \tag{13}$$

where the equality means that both sides have the same distribution.

We can deduce exact spectra for the Π_H motion if we use discrete wavelet bases. Wavelets are generally associated with time-scale representations. Let f be a $L^2(\mathbb{R})$ function. It is shown in Ref. [36] the existence of complete sets $\{\psi_{jn}\}$ such that f can be expanded as

$$f(t) = \sum_{j=-\infty}^{j=\infty} \sum_{n=-\infty}^{n=\infty} a_{jn} \psi_{jn}(t), \tag{14}$$

the form of the functions ψ_{nj} being

$$\psi_{jn}(t) = \frac{1}{\sqrt{2^j}} \psi\left(\frac{t - 2^j n}{2^j}\right). \tag{15}$$

These functions are called discrete wavelets, and are square integrable with zero mean, at least. The function ψ generating the wavelets is called the mother wavelet. Often, classes of wavelets are employed which are orthogonal to polynomials up to a certain degree k, with the purpose of detrending data, and studying singularities; k is the number of vanishing moments of the wavelet. The set $\{\psi_{jn}\}$ is a wavelet basis, and the discrete wavelet transform of f to this basis is written

$$a_{jn} = D_{jn} f = \langle \psi_{jn}|f\rangle, \tag{16}$$

and gives information on the behavior of the function f at scale 2^j and time $2^j n$.

It is possible to work with restrictions of the considered motions as $L^2(I)$ functions, with $I \subset \mathbb{R}, I \neq \mathbb{R}$. We make such restrictions by noting that experiments or simulations get data during a time T, with a sample interval τ, so that the number of sample points is $N = T/\tau$. For convenience, we make $T = 1$, and $\tau = 1/N = 2^{-J}$. Using this information in expression (14), and assuming compact support for the wavelets, we can write

$$\pi_H(t) = a_\phi \phi(t) + \sum_{j=-J+1}^{j=0} \sum_{n=0}^{n=2^{-j}-1} a_{jn} \psi_{jn}(t), \tag{17}$$

where π_H is the restriction of Π_H to $[0,1]$, $a_\phi \equiv \langle \phi|\pi_H\rangle$, and the function ϕ is defined as the linear combination

$$\phi(t) = \sum_{j=1}^{j=\infty} c_j \psi_{j0}(t) \tag{18}$$

that can be determined from its Fourier transform

$$\hat{\phi}(\omega) = \frac{\sqrt{2}}{\hat{g}(\omega)} \hat{\psi}(2\omega). \tag{19}$$

Here g is the high pass mirror filter associated with the corresponding multiresolution [36]. In expression (18), the functions ψ_{j0} were also conveniently restricted to the interval $[0,1]$. The function ϕ is called the scaling function.

We will now use Haar wavelet basis to calculate an exact wavelet spectrum for Π_H. The Haar wavelets are periods of square waves written as

$$h_{jn}(t) = \frac{1}{\sqrt{2^j}} \begin{cases} 1, & t \in I_{jn}^1 \\ -1, & t \in I_{jn}^2, \end{cases} \tag{20}$$

where

$$I_{jn}^1 = [2^j n, 2^j (n + 1/2)],$$

$$I_{jn}^2 = [2^j (n + 1/2), 2^j (n+1)]. \tag{21}$$

For Haar wavelets, one proves, using the expressions (11) and (20), that

$$\sigma_j^2(H)=\overline{|\Delta_{jn}\Pi_H|^2}=C_H 2^{(2H+1)j}, \tag{22}$$

where $\Delta_{jn}f\equiv\langle h_{jn}|f\rangle$ and

$$C_H=\frac{\sigma_H^2(1-2^{-2H})}{(2H+1)(2H+2)}. \tag{23}$$

Expression (22) gives us the scale dependent power spectrum in the Haar basis. Note that if an effective frequency $|\omega|^{-1}\equiv 2^j$ is substituted, one finds the expected $1/|\omega|^{2H+1}$ relation. Except for the constant, this spectrum has the same well behaved dependence on scale for Π_H using any discrete wavelet (see Refs. [36,37], and references therein for more details on this aspect).

At every scale 2^j, we can look at the distribution P_j of the coefficients a_{jn}. For the monofractals, P_j collapses to a unique probability distribution, after the coefficients are normalized by the standard deviation σ_j. In other situations, this is not so because the only constraint expression (22) gives is on the second moments of these distributions. So we have a great latitude to choose models presenting multifractality, without affecting the correlations that are essentially linked to H by the expression (11). However, there is the question: what are the general conditions on P_j in order that the series (17) be convergent, when $J\to\infty$?

The convergence issue is directly related with the statistics of rare high valued fluctuations. If they are too frequent, we can have divergence caused by their repeated occurrence in the sum. The probability of the event set Ω_j of such rare fluctuations can be calculated for each scale j as

$$r_j=\int_{-\infty}^{-a_j} dx\, P_j(x)+\int_{a_j}^{\infty} dx\, P_j(x), \tag{24}$$

with $a_j\equiv m\sigma_j$, m being a natural number as big as one needs. Now the condition for convergence can be expressed using the Borel-Cantelli lemma. If

$$\sum_{j=-\infty}^{0} r_j<\infty, \tag{25}$$

then Prob(Ω_j, infinitely often)$=0$. In such a case, for almost all realizations, there is a maximum absolute value for the coefficients which does not exceed a_j. In consequence,

$$\sum_j \sum_n a_{jn}^2 \leqslant \sum_j a_j^2 = m^2 C_H \sum_j 2^{(2H+1)j}<\infty, \tag{26}$$

which proves convergence [33].

It remains to see in which cases the condition for convergence is valid. Using the expressions (24) and (25), one draws the conclusion that the convergence happens if, and only if, the function

$$F(x)\equiv\sum_j P_j(x) \tag{27}$$

is integrable in both intervals $(-\infty,-a_j]$ and $[a_j,\infty)$. The fulfillment of this equivalent condition depends on the decay

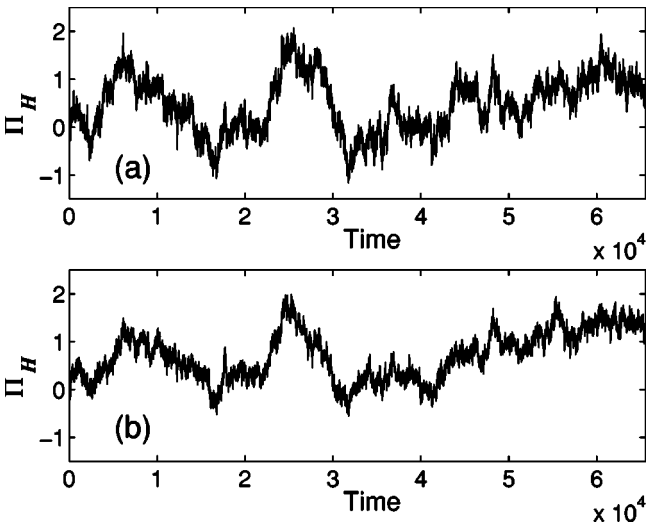

FIG. 1. Monofractal (a) and multifractal (b) motions generated with SRA and mSRA algorithms. These samples have 2^{16} points and were produced with the same seed for the random number generator, and correspond to sample number 15 from the 50 generated in each group.

of the functions P_j. Among all these functions, we can single out the one with the slowest decay when $x\to\infty$, noted as F^+, and that with the slowest decay when $x\to-\infty$, noted as F^-. For the rare events, the function F behaves asymptotically as F^+ or F^-. Thus, the smallest acceptable decay for these last functions, in order that convergence occurs is

$$F^+(x)\sim\frac{1}{x^{1+\varepsilon^+}},\quad F^-(x)\sim\frac{1}{(-x)^{1+\varepsilon^-}}, \tag{28}$$

with $\varepsilon^{\pm}>0$ being small numbers. Following this result, we assume that no P_j decays slower than that indicated in the above expression. This assumption allows for a number of physically important cases, as the ones presenting exponential tails, not to speak of the Gaussian case (fBm) [21,22,26].

The literature is plenty of works, in which Hurst exponents are used to characterize complex motions. The above discussion indicates that, with great generality, these exponents are only connected with the scaling of second moments, and this is the only information that can be drawn from linear fits. The fact is that with this single measurement, one has very few interpretive elements on the physics of the process because one cannot determine the degree of symmetry involved. The physical process generating a fractal motion must be much simpler, due to the self-affinity, than in the multifractal case, where something (P_j) does change with scale. Since by the value of the Hurst exponent one cannot quantify the symmetry breaking effect that is taking place, no precise judgment can be made about the scaling, and in consequence about its implications for the mechanisms of the process. *Ulterior* information can be obtained by considering the probability distributions of discrete wavelet coefficients. The minimum gain with this simple procedure is to clarify the properties of the complex motion. To have this point clear, consider Fig. 1. There one finds in (a) a

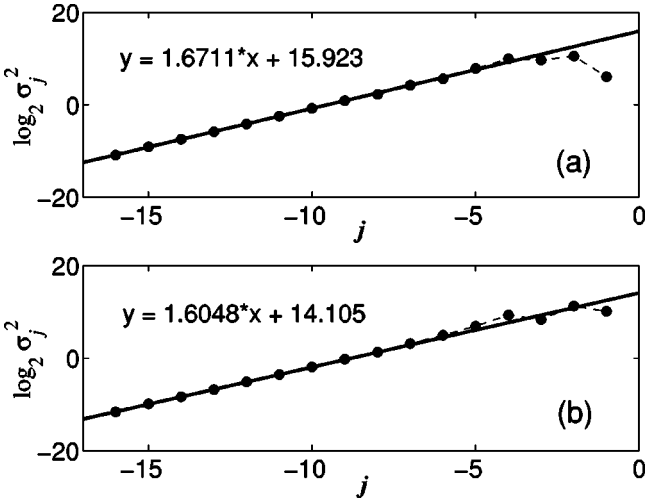

FIG. 2. Linear fits for the second moment of the wavelet coefficients. In (a) for sample number 15 of the SRA group, and in (b) for sample number 15 of the mSRA group.

sample of fBm generated using the successive random additions (SRA) method [38]. The data for (b) is from a modified version that generates multifractals called here the multifractal SRA (mSRA). The data for the fractals and multifractals were generated using the same seeds for the random number generator, and those in the figures are numbered 15 of a total of 50 samples in each group. All 100 samples have 2^{16} points. Figure 2 contains two high quality linear fits of $\log_2\sigma_j^2$ versus j, one for each of the selected samples. These plots allow one to find the Hurst exponent using expression (22). A result of such estimate for all samples is shown in Fig. 3. The excellent fit presented does not quantify or qualify the reported origins (SRA and mSRA) of the two groups, except for the fact that they have diverse, though near, values for the Hurst exponent.

The probability densities P_j of discrete wavelet coefficients are shown in Fig. 4 for the monofractals and in Fig. 5

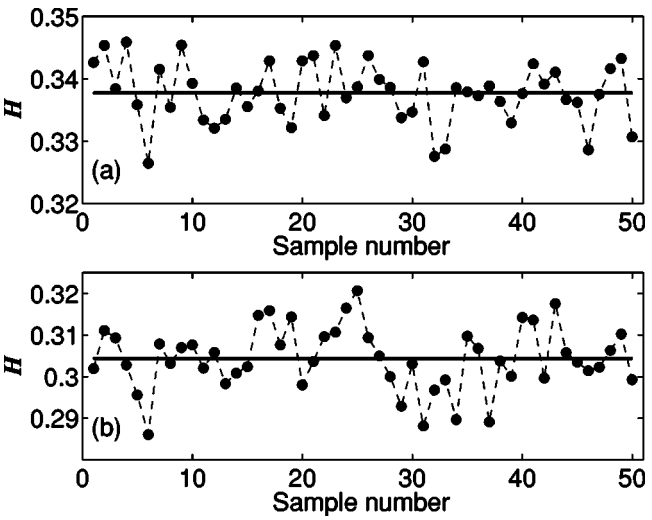

FIG. 3. Hurst exponents for all samples generated. The exponents were calculated using expression (22). Those in (a) correspond to the SRA group, and those in (b) to the mSRA group.

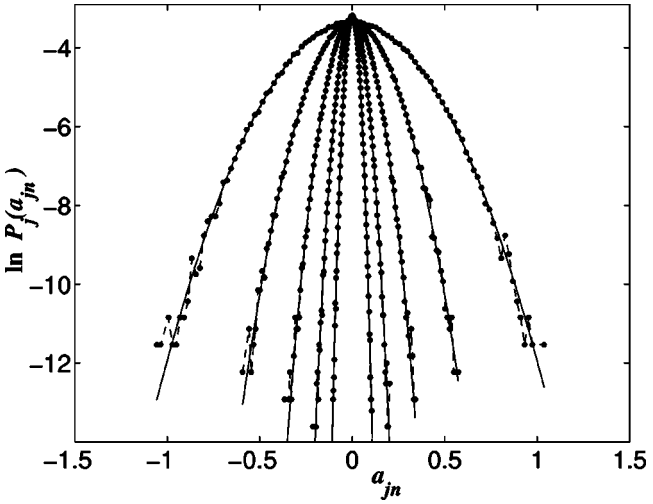

FIG. 4. Probability distributions P_j of the wavelet coefficients a_{jn} in a semilog graph, for the group generated with the SRA algorithm. The parabolas are Gaussians with the same variance of the distributions.

for the multifractals. These statistics were obtained from the wavelet coefficients of all samples in each group, and the differences are noticeable. In Fig. 4, the data is well represented by Gaussians (appearing in the semilog graph as parabolas) with the same variances of the determined PDFs, making clear that the first group is self-affine symmetric. In Fig. 5, exponential tails appear showing that the PDFs have a smaller decay if compared with the Gaussian case (intermittency appears). In Fig. 6, the variation of the kurtosis of the probability distributions with the scale is shown for the monofractal and multifractal cases. As expected, the multifractals have pronounced variation with scale. So this group presents only a weak self-affinity given by expression (12). Now one can be sure that the data were not produced through the same mechanisms (in our case, algorithms) or that the

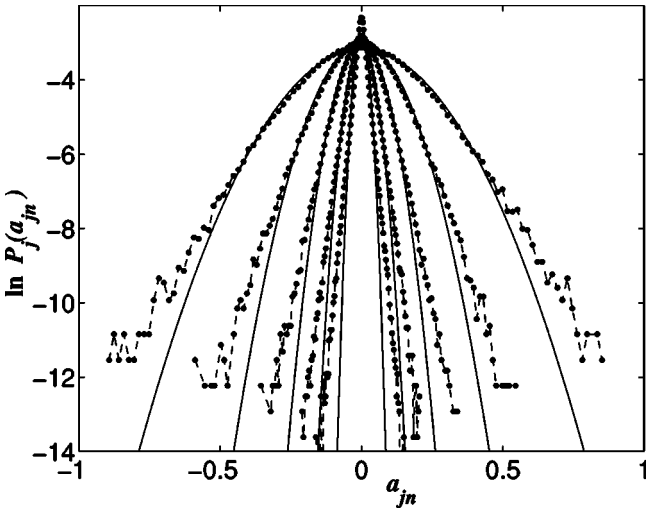

FIG. 5. Probability distributions P_j of the wavelet coefficients a_{jn} in a semilog graph, for the group generated with the mSRA algorithm. The parabolas are Gaussians with the same variance of the distributions. Note the increase in the probability of high fluctuations.

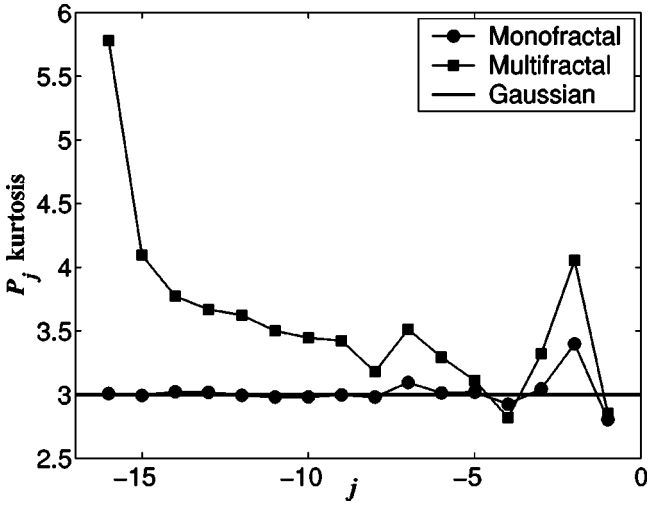

FIG. 6. Kurtosis of probability distributions P_j of the wavelet coefficients a_{jn} in a semilog graph, for the monofractals and for the multifractals. The kurtosis for the multifractals presents pronounced variation, indicating change of the distribution with scale.

system was not in the same regime when they were measured. What is interesting is that this certainty is reached at very low cost because just a fast wavelet transform (FWT), an $O(n)$ algorithm, is used to obtain the discrete wavelet coefficients. It is important to mention that one can also use the FWT to estimate the singularity spectrum $D(h)$, even though the more precise wavelet formalism to this end is based on the CWT. The essence of the procedure remains all the same as the referred method, except that instead of the maxima line representation one uses a discrete wavelet representation, with gain in efficiency, which can be helpful for large data. We do not go further on this issue because extensive information can be found elsewhere [25,29,30,33].

III. MULTIFRACTAL HYPERSURFACES

We will now proceed with the generalization of the previously discussed motion to d dimensions. The important new element introduced when $d>1$ is direction. We have seen that in one dimension, it is possible to make an association of every process f with an incremental process μ_f. In higher dimensions, the straightforward generalization of μ_f is a quantity $\mu_{f,\hat{\mathbf{u}}}$ which, in general, depends on the direction through the unit vector $\hat{\mathbf{u}}$. After that, we can use the multifractal formalism to find direction dependent singularity spectra. The incremental process now scales as $\mu_{f,\hat{\mathbf{u}}} \sim l^{h(\mathbf{x},\hat{\mathbf{u}})}$, and the sets of fractals corresponding to this multifractal are $S_{h,\hat{\mathbf{u}}}=\{\mathbf{x}\in S: h(\mathbf{x},\hat{\mathbf{u}})=h\}$, where S is the support. So, an appropriate generalization of the $D(h)$ singularity spectrum is a function $D(h,\hat{\mathbf{u}})$ for the scaling exponent of the sets $S_{\alpha,\hat{\mathbf{u}}}$. This spectrum takes into account the regularity of f, including direction effects (compare with the formulation in Ref. [32]). The Hölder exponents correspond to the dominant scaling of the function at a point and can be found from $h(\mathbf{x},\hat{\mathbf{u}})$ using the relation

$$h(\mathbf{x}) \equiv \min_{\hat{\mathbf{u}}} h(\mathbf{x},\hat{\mathbf{u}}). \tag{29}$$

Following this logic, the problem of finding the $h(\mathbf{x},\hat{\mathbf{u}})$ spectrum reduces to that of finding the scaling of all unequal sets $S_{\alpha,\hat{\mathbf{u}}}$. A multifractal function is then characterized by the existence of such unequal sets. In particular, one can have the situation in which the Hölder exponent $h(\mathbf{x})$ is homogeneous, but the direction associated to it varies from point to point in a complicated manner. A cut through such a hypersurface would reveal its multifractal nature that is not manifested by using the $D(h)$ spectrum only.

We suggest here the need of this complete directionality for a full characterization of the spectra of hypersurfaces. This can be achieved by using a direct generalization of the structure function method, in which $\delta_{l,\hat{\mathbf{u}}} f(\mathbf{x}) \equiv f(\mathbf{x}+l\hat{\mathbf{u}}) - f(\mathbf{x})$, and one searches for the scaling exponents $\zeta_{q,\hat{\mathbf{u}}}$ of

$$S_{q,\hat{\mathbf{u}}}(l) \equiv \int d^d\mathbf{x} |\delta_{l,\hat{\mathbf{u}}} f(\mathbf{x})|^q, \tag{30}$$

when $l\to 0$. The wavelet method can be generalized by considering the transform

$$W_{l,\mathbf{x}_0,\hat{\mathbf{u}}} f(\mathbf{x}) \equiv \int d^d\mathbf{x}\, \psi_{l,\mathbf{x}_0,\hat{\mathbf{u}}}(\mathbf{x})\, f(\mathbf{x}) \tag{31}$$

with

$$\psi_{l,\mathbf{x}_0,\hat{\mathbf{u}}}(\mathbf{x}) \equiv \hat{\mathbf{u}}\cdot\nabla\left[\frac{1}{\sqrt{l}}\Phi\left(\frac{\mathbf{x}-\mathbf{x}_0}{l}\right)\right]. \tag{32}$$

The function Φ is a smoothing kernel. The partition function is then written

$$Z_{q,\hat{\mathbf{u}}}(l) \equiv \sum \max|\langle \psi_{l,\mathbf{x}_0,\hat{\mathbf{u}}}| f\rangle|^q, \tag{33}$$

which scales with exponent $\tau_{q,\hat{\mathbf{u}}}$ (the sum is on the support of the local maxima of the modulus of the wavelet transform). Observe that, as far as there are only point singularities, there is no degeneracy of the is maxima. In each scale they are countable, so that the sum in expression (33) is well defined. The case with line singularities or more complex degenerate singularities are not appropriately dealt using wavelets (for the sake of spectral characterization). Probably, a correct way to take into account these situations is by using analyzing functions such as ridgelets or curvelets [39,40].

In the explained context, a multifractal function is characterized by the existence of nonlinear $\zeta_{q,\hat{\mathbf{u}}}$ or $\tau_{q,\hat{\mathbf{u}}}$, for some direction $\hat{\mathbf{u}}$. When these exponents are linear functions of q but vary with direction, we have only the anisotropy of the scaling properties. The Legendre transforms from which one calculates the $D(h,\hat{\mathbf{u}})$ spectrum are

$$D(h,\hat{\mathbf{u}}) = \min_q (qh - \zeta_{q,\hat{\mathbf{u}}} + d), \tag{34}$$

or

$$D(h,\hat{\mathbf{u}}) = \min_q (qh - \tau_{q,\hat{\mathbf{u}}}). \tag{35}$$

Let us now introduce, using the inverse discrete wavelet transform, a class of multifractal hypersurfaces corresponding to the multifractal motion studied in the Sec. II. A suitable point of departure is the known spectrum for the fBm in d dimensions,

$$S(\omega) \sim \frac{1}{|\omega|^{2H+d}}. \tag{36}$$

From this spectrum, we expect that the second moments of the wavelet coefficients scale as $2^{(2H+d)j}$. To generate an fBm in d dimensions, one just needs to produce the wavelet coefficients with the Gaussian distributions at every scale having variances proportional to $2^{(2H+d)j}$, then transform to the real space.

Along the same line, we define the $\Pi_{\mathbf{H}}(\mathbf{x})$ hypersurface, where $\mathbf{x}=(x_1, \ldots, x_d)$, from wavelet coefficients. This can be formalized as follows. The d dimensional discrete wavelets are functions having the form

$$\psi^{\varepsilon}_{jn}(\mathbf{x}) = \frac{1}{\sqrt{2^{dj}}} \psi^{\varepsilon}\left(\frac{x_1 - 2^j n_1}{2^j}, \ldots, \frac{x_d - 2^j n_d}{2^j} \right), \tag{37}$$

where $\mathbf{n} \equiv (n_1, \ldots, n_d) \in \mathbb{Z}^d$, and

$$\psi^{\varepsilon} \equiv \psi^{\varepsilon_1} \cdots \psi^{\varepsilon_d}, \tag{38}$$

with $\varepsilon \equiv (\varepsilon_1, \ldots, \varepsilon_d) \in \{0,1\}^d$ being a direction index. The function $\psi^0 \equiv \phi$, a one-dimensional scaling function corresponding to a one-dimensional discrete wavelet basis, and $\psi^1 \equiv \psi$ is the mother wavelet. This construction provides a separable orthonormal wavelet basis for the space $L^2(\mathbb{R}^d)$ [36]. The order of the ε indices is given by the natural sequence of the corresponding binary numbers. When $\varepsilon = 0$, ψ^{ε} is the d-dimensional scaling function. The $(2^d - 1)$ functions formed when $\varepsilon \neq 0$ are the d-dimensional mother wavelets. Let p be the number of $1s$ in a ε index. The number $g \equiv p - 1$, $p \geq 1$ specifies the diagonal character of the associated mother wavelet, so that $g = 0$ means the wavelet does not follow a diagonal, for $g = 1$, it is oriented along a diagonal of a square, for $g = 2$, it is oriented along a diagonal of a cube, and so on.

The hypersurface $\Pi_{\mathbf{H}}(\mathbf{x})$ is now defined through the infinite series

$$\Pi_{\mathbf{H}}(\mathbf{x}) \equiv \sum_j \sum_n \sum_{\varepsilon} a^{\varepsilon}_{jn} \psi^{\varepsilon}_{jn}, \tag{39}$$

where the coefficients a^{ε}_{jn} are distributed according the PDFs P^{ε}_j, where $\varepsilon \neq 0$. In $d > 1$ dimensions, there is more freedom when putting conditions on these PDFs than in one dimension. Here we may also have the situation in which different directions have different values of H. Accordingly, we define the index $\mathbf{H} \equiv (H_1, \ldots, H_{2^d-1})$ such that there is one value of H for each wavelet orientation. This is a natural way to introduce anisotropy in the hypersurfaces. The condition on the second moments of the distributions P^{ε}_j is generalized to

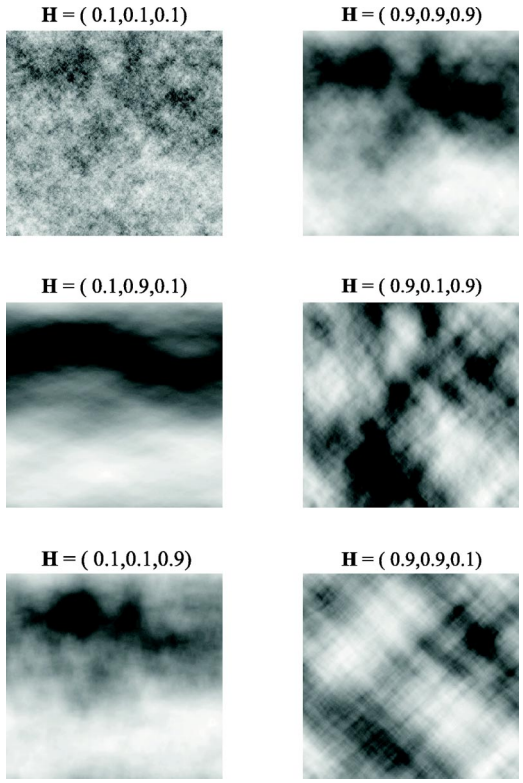

FIG. 7. Fractal surfaces generated by inverse FWT. The resolution is $N = 512$ in all cases. The Hurst exponents are given by $\mathbf{H} = (H_{01}, H_{10}, H_{11})$. The first row presents the isotropic strongly anticorrelated and strongly correlated cases. The second row mixes correlation and anticorrelation, with contrasting Hurst exponent in the vertical direction. In the third row, the contrast is in the diagonal.

$$\overline{|a^{\varepsilon}_{jn}|^2} \sim 2^{(2H_{\varepsilon}+d)j}. \tag{40}$$

Finally, we note that, to assure the convergence of the series, the PDFs of the coefficients must be subjected to the same condition as in the one-dimensional case. The proof is easily done by considering each direction separately, and using the same argument given in Sec. II.

Figure 7 shows examples of anisotropic bidimensional fBm obtained with this method. The probability distributions P^{ε}_j are Gaussians. Following the assumed ordering, $H_1 = H_{01}$ is related to the horizontal, $H_2 = H_{10}$ to the vertical, and $H_3 = H_{11}$ to the diagonal. The first row has one case of strongly anticorrelated fBm, followed by a strongly correlated fBm, that are isotropic. In the second and third rows, one sees the results of introducing anisotropy by mixing strong correlation and anticorrelation. In the second row, the vertical direction has the contrasting Hurst exponent. In the third row, this role is played by the diagonal. This figure provides some illustration of the possible textures obtained in limiting conditions, but it is clear that all intermediate combinations are possible in practice.

IV. CONCLUSION

We have discussed the use of the discrete wavelet transform as a means to produce computer generated multifractal hypersurfaces. These multifractals present a correlation structure similar to the fBm, and can be anisotropic. They are expected to be useful in areas where stochastic fields with long range correlations are employed, e.g., in the geostatistics of large scale porous media [41], in growth phenomena [42,43], in turbulence [27,44], and in economics [45]. We also point the possibility of using this kind of technique as a powerful method for characterization of scaling in general. Our examples show how one can obtain information on effects that break an exact self-similarity or self-affinity. The methodology could even be carried to cases where scale breaks dominate scaling, as for example, when considering the seafloor surface [46].

ACKNOWLEDGMENTS

We would like to thank Professor A. Arnéodo and Professor F.J. Herrmann for their lectures on multifractals and wavelets given at UFRN. We acknowledge CAPES, CNPq, FINEP, and CTPETRO for financial support.

[1] B. B. Mandelbrot, *The Fractal Geometry of Nature* (Freeman, San Francisco, 1982).
[2] *Fractals in Science*, edited by A. Bunde and S. Havlin (Springer-Verlag, Berlin, 1998).
[3] D. Stauffer and A. Aharony, *Introduction to Percolation Theory*, 2nd ed. (Taylor and Francis, London, 1994).
[4] M. Sahimi, *Flow and Transport in Porous Media and Fractured Rock* (VHC, Weinheim, 1995).
[5] A.N. Kolmogorov, C. R. Acad. Sci. URSS **30**, 301 (1941).
[6] U. Frish, Proc. R. Soc. London, Ser. A **434**, 89 (1991).
[7] P. Grassberger and I. Procaccia, Phys. Rev. Lett. **50**, 346 (1983).
[8] R. Badii and A. Politi, Phys. Rev. Lett. **52**, 1661 (1984).
[9] Y. Termonia and Z. Alexandrowicz, Phys. Rev. Lett. **51**, 1265 (1983).
[10] T.A. Witten, Jr. and L.M. Sander, Phys. Rev. Lett. **47**, 1400 (1981).
[11] J.P. Flory, J. Am. Chem. Soc. **63**, 3083 (1941).
[12] D.J. Wilkinson and J. Willemsen, J. Phys. A **16**, 3365 (1983).
[13] B.B. Mandelbrot and J.W. Van Ness, SIAM Rev. **10**, 422 (1968).
[14] H.G.E. Hentschel and I. Procaccia, Phys. Rev. A **29**, 1461 (1984).
[15] R. Blumenfeld *et al.*, Phys. Rev. B **35**, 3524 (1987).
[16] A.L. Barabási *et al.*, Phys. Rev. A **45**, R6951 (1992).
[17] A.L. Barabási and T. Vicsek, Phys. Rev. A **44**, 2730 (1991).
[18] T.C. Halsey, P. Meakin, and I. Procaccia, Phys. Rev. Lett. **56**, 854 (1986).
[19] C. Amitrano, A. Coniglio, and F. di Liberto, Phys. Rev. Lett. **57**, 1016 (1986).
[20] H.G.E. Hentschel, Phys. Rev. E **50**, 243 (1994).
[21] B.I. Shraiman and E.D. Siggia, Nature (London) **405**, 639 (2000).
[22] Jayesh and Z. Warhaft, Phys. Rev. Lett. **67**, 3503 (1991).
[23] J. Paret and P. Tabeling, Phys. Fluids **10**, 3136 (1998).
[24] S. Roux, J.F. Muzy, and A. Arnéodo, Eur. Phys. J. B **8**, 301 (1999).
[25] N. Decoster, S.G. Roux, and A. Arnéodo, Eur. Phys. J. B **15**, 739 (2000).
[26] S.G. Roux, A. Arnéodo, and N. Decoster, Eur. Phys. J. B **15**, 765 (2000).
[27] U. Frish and G. Parisi, in *Turbulence and Predictability of Geophysical Flows and Climate Dynamics*, Proceedings of the International School of Physics ''Enrico Fermi,'' Course 88, edited by M. Ghil, R. Benzi, and G. Parisi (North-Holland, New York, 1985).
[28] T. C. Halsey *et al.*, Phys. Rev. A **33**, 1141 (1986).
[29] A. Arnéodo, E. Bacry, and J. F. Muzy, Physica A **213**, 232 (1995).
[30] J.F. Muzy, E. Bacry, and A. Arnéodo, Int. J. Bifurcation Chaos **4**, 245 (1994).
[31] J.F. Muzy, E. Bacry, and A. Arnéodo, Phys. Rev. E **47**, 875 (1993).
[32] A. Arnéodo, N. Decoster, and S.G. Roux, Eur. Phys. J. B **15**, 567 (2000).
[33] A. Arnéodo, E. Bacry, and J.F. Muzy, J. Math. Phys. **29**, 4142 (1998).
[34] S. Jaffard, SIAM (Soc. Ind. Appl. Math.) J. Math. Anal. **28**, 944 (1997).
[35] S. Jaffard, SIAM (Soc. Ind. Appl. Math.) J. Math. Anal. **28**, 971 (1997).
[36] S. Mallat, *A Wavelet Tour of Signal Processing*, 2nd ed. (Academic Press, Boston, 1998).
[37] A. Coron, P. Flandrin, and N. Gache, in *1998 IEEE-SP International Symposium on Time-Frequency and Time-Scale Analysis, Pittsburgh* (IEEE Standards Office, New York, 1998), pp. 361–364.
[38] *The Science of Fractal Images*, edited by H. O. Peitgen and D. Saupe (Springer-Verlag, New York, 1987).
[39] E.J. Candès and D.L. Donoho, Philos. Trans. R. Soc. London, Ser. A **357**, 2495 (1999).
[40] E. J. Candès and D. L. Donoho, in *Curve and Surface Fitting*, edited by A. Cohen, C. Rabut, and L. L. Schumaker (Vanderbilt University Press, Nashville, 2000).
[41] D. M. Tavares and L. S. Lucena (unpublished).
[42] A. L. Barabási and H. E. Stanley, *Fractal Concepts in Surface Growth* (Cambridge University Press, Cambridge, 1995).
[43] T. Vicsek, *Fractal Growth Phenomena* (World Scientific, Singapore, 1989).
[44] B. B. Mandelbrot, *Multifractals and* $1/f$ *Noises* (Springer, New York, 1998).
[45] B. B. Mandelbrot, *Fractals and Scaling in Finance* (Springer, New York, 1997).
[46] U.C. Herzfelt and C. Overbeck, Comput. Geosci. **25**, 979 (1999).